Domains of Mnt Repressor: Roles in Tetramer Formation, Protein Stability, and Operator DNA Binding†

Carey D. Waldburger and Robert T. Sauer*

Department of Biology, Massachusetts Institute of Technology, Cambridge, Massachusetts 02139

Received April 3, 1995; Revised Manuscript Received June 29, 1995⊗

ABSTRACT: The Mnt repressor of bacteriophage P22 is a member of the ribbon−helix−helix family of gene regulatory proteins. Proteolytic cleavage of Mnt with chymotrypsin reveals that it consists of two structural domains. Both domains are required for high-affinity operator binding. The N domain (residues 1−51) is dimeric and binds weakly but specifically to operator DNA. The C domain (residues 52−82) forms an independent α-helical, tetramerization domain and, by itself, has no DNA−binding activity. In intact Mnt, the N and C domains help to stabilize each other against denaturation but appear to be linked rather flexibly. Assays of the half-operator affinities of Mnt and the isolated N domain indicate that binding to adjacent half-sites in the whole operator is stabilized by protein−protein contacts between N domains in addition to protein−protein contacts between C domains.

A common theme in protein structure and function is the use of independent domains to perform separate but interrelated tasks. This is especially true of transcription factors, where the activities of individual DNA-binding units are frequently coupled by separate oligomerization domains. The ability of such proteins to form homo- or hetero-oligomers can be critical to both the specificity and strength of DNA binding. Thus, understanding and characterizing how oligomerization domains contribute to function is important in furthering our understanding of protein−DNA recognition.

Bacteriophage P22 encodes two repressors, Mnt and Arc, which regulate transcription in the immunity I region [for review, see Susskind and Youderian (1983)]. Mnt negatively regulates transcription of the *arc* and *antirepressor* genes during lysogenic growth of the prophage, while Arc represses transcription of these genes and *mnt* during lytic phage growth. Each protein binds as a tetramer to a distinct 21-base-pair operator site, but Arc is a dimer in solution while Mnt is a tetramer (Vershon *et al.*, 1985, 1987a,b; Brown *et al.*, 1990). As shown in Figure 1, many residues in the N-terminal two-thirds of Mnt are homologous with those in Arc, while the C-terminal one-third of the Mnt sequence is not present in Arc (Sauer *et al.*, 1983). The structures of Arc (Breg *et al.*, 1990; Bonvin *et al.*, 1994) and of a dimeric variant of Mnt lacking six C-terminal residues (Mnt_{1-76}; Burgering *et al.*, 1994) reveal that the homologous regions of the two proteins have similar three-dimensional folds, consisting of a β-ribbon and two α-helices. The β-strands pair to form a β-sheet which packs against the α-helices to form a roughly globular structure (Figure 1). In the dimeric Mnt_{1-76} mutant, the ribbon−helix−helix fold comprises residues 5−43 and is followed by a loop region, a metastable third helix (residues 54−66), and a random coil region (Burgering *et al.*, 1994). Unlike wild-type Mnt, the truncated Mnt_{1-76} mutant does not form tetramers and binds operator DNA only weakly (Knight & Sauer, 1988). These observations suggest that the C-terminal residues of Mnt are involved in tetramer formation and that tetramer formation is important for DNA binding. There is currently no direct structural information about the Mnt−operator complex, but the cocrystal structure of the Arc complex (Raumann *et al.*, 1994) can be used as a model because footprinting and hybrid protein studies indicate that the two complexes must be very similar (Vershon *et al.*, 1987a,b; Knight & Sauer, 1989). In the Arc complex, dimers interact with adjacent operator half-sites using the β-sheet for major groove contacts, and the DNA-bound tetramer is stabilized by a small number of cooperative interactions between the dimers.

Here, we show that Mnt contains two structural domains. The N domain folds as a dimer, binds weakly to an operator half-site, and binds cooperatively and more avidly to the intact operator. The C domain forms an independent, α-helical, tetramerization domain. Comparing the DNA-binding properties of Mnt and the isolated N domain suggests that binding to operator DNA is influenced by two distinct types of protein−protein interactions, involving contacts between N-domain dimers at one level and contacts between subunits of the C-domain tetramer at the second level.

MATERIALS AND METHODS

Buffers and Reagents. Buffer A is 0.1 M sodium phosphate (pH 8.0), 10 mM Tris·HCl (pH 8.0), 3 mM imidazole, and 6 M guanidine hydrochloride. Buffer B is 10 mM Tris·HCl (pH 7.5) and 1 mM EDTA. Storage buffer (SB) is 50 mM Tris·HCl (pH 7.5), 0.25 M KCl, and 0.2 mM EDTA. Phosphate buffer (PB) is 50 mM sodium phosphate (pH 7.5) and 0.2 M KCl. Gel filtration buffer is 6 M guanidine hydrochloride, 0.15 M KCl, and 0.1 mM EDTA. Footprinting buffer is 30 mM HEPES−KOH (pH 7.5), 0.1 M potassium glutamate, 10 mM $MgCl_2$, 1.5 mM $CaCl_2$, 0.1 mM EDTA, 100 μg/mL bovine serum albumin, and 0.02% Nonidet P-40. Binding buffer is identical to footprinting buffer except 30 mM Tris·HCl (pH 7.5) was substituted for HEPES·KOH.

Proteins and Peptide Fragments. Purified Mnt protein was a gift from B. Raumann. A gene-encoding Mnt with six histidines added to the C terminus (*mnt-st6*) was

† This work was supported by NIH Grant AI-16892 and by a postdoctoral fellowship to C.D.W. from the NIH.

⊗ Abstract published in *Advance ACS Abstracts,* September 15, 1995.

0006-2960/95/0434-13109$09.00/0

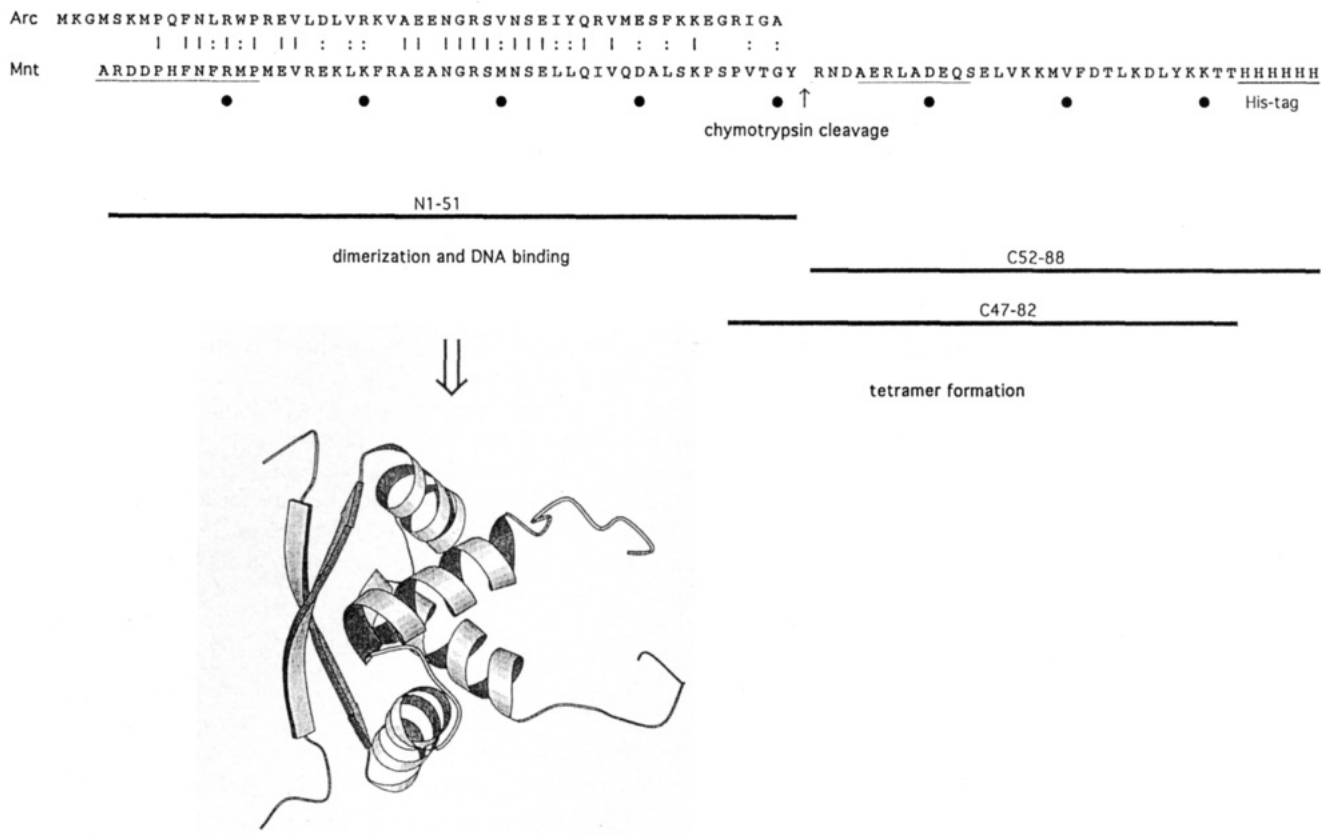

FIGURE 1: Amino acid sequences of Mnt-st6 and Arc. Positions of sequence identity or similarity are marked. The H_6 sequence underlined at the C terminus of Mnt-st6 is not present in normal Mnt. The other underlined sequences match those determined by sequential Edman degradation of the N_{1-51} and C_{52-88} fragments. The site of chymotryptic cleavage is shown, as are the relative positions of the N- and C-terminal fragments studied in this paper. The ribbon representation of the N domain (residues 1−51) of Mnt is from the NMR structure of the dimeric Mnt_{1-76} mutant (Burgering *et al.*, 1994) using coordinates provided by R. Boelens and R. Kaptein.

constructed by cloning a cassette with the sequence 5′-GGATTTGTACAAGAAGACCACCCACCAC-CACCACCACCACTGATTA-3′ between *Afl*II and *Nsi*I sites in pTM203. Plasmid pTM203 is a pBR322-based derivative of pTM201 (Vershon *et al.*, 1985), in which *Afl*II and *Nsi*I sites have been created by a C·G → A·T change at the third position of *mnt* codon 74 and by an A·T → T·A change in a noncoding region 15 base pairs downstream from the *mnt* stop codon, respectively. The Mnt-st6 protein was purified from *Escherichia coli* strain X90 (Amman et al., 1983) transformed with plasmid pTM203-st6 by nickel-chelate chromatography essentially as described by Milla and Sauer (1993). Cells expressing Mnt-st6 from the *tac* promoter were induced with 1 mM IPTG, harvested, resuspended in buffer A, and lysed as described (Milla & Sauer, 1993). Cellular debris was removed by centrifugation, and the supernatant was passed over a Ni^{2+}−NTA metal-chelate column (Qiagen, Inc.). The resin was washed with 200 mL of buffer A, and Mnt-st6 was eluted with 0.2 M acetic acid/6.0 M guanidine hydrochloride. Following dialysis into buffer B, the protein was loaded onto a SP-Sephadex (Pharmacia) cation-exchange column, washed with 100 mL of buffer B, and eluted with buffer B plus 2 M NaCl. The protein was dialyzed against SB and judged to be greater than 95% pure by Coomassie blue staining of a sample following electrophoresis on a 15% Tris−Tricine gel (Schagger & von Jagow, 1987). The protein concentration (in moles of monomer equivalents per liter) was calculated using an extinction coefficient of 2394 M^{-1} cm^{-1} at 280 nm based on the presence of two tyrosines in the sequence (Fasman, 1975).

Mnt and Mnt-st6 were subjected to limited proteolysis by incubation with chymotrypsin (E/S = 1/500 M/M) for 1 h at 22 °C in SB. After the reaction was stopped by addition of phenylmethylsulfonylfluoride (2 mM final concentration), analysis by gel electrophoresis showed residual intact protein and two cleavage fragments (see Results). For Mnt-st6, the His6-tagged intact protein and the C-terminal fragment (C_{52-88}) were separated from the N-terminal fragment (N_{1-51}) by nickel-chelate chromatography essentially as described above. Uncleaved Mnt-st6 and the C_{52-88} fragment were then separated by FPLC gel filtration using a Superdex HR75 column (Pharmacia). Fractions containing C_{52-88} were pooled, dialyzed against 50 mM ammonium bicarbonate, and lyophilized. Amino-terminal sequencing and amino acid analysis of the N_{1-51} and C_{52-88} fragments were performed by the MIT Biopolymers lab.

An N-terminal acetylated peptide corresponding to the C-terminal 36 amino acids of wild-type Mnt (C_{47-82}) was synthesized and purified by reverse-phase HPLC by the MIT Biopolymers lab. The concentrations of N_{1-51} and C_{52-88} (in moles of monomer equivalents) were calculated using an extinction coefficient at 280 nm of 1197 M^{-1} cm^{-1} (one tyrosine each), and that of C_{47-82} was calculated using an extinction coefficient at 280 nm of 2394 M^{-1} cm^{-1} (two tyrosines) (Fasman, 1975).

Measurement of Secondary Structure and Protein Stability. Circular dichroism (CD) measurements were performed using an AVIV 60DS instrument equipped with a Hewlett Packard 89110A temperature-controlled sample holder. Fractional α-helicity was calculated from CD spectra as described by

Chen *et al.* (1972). Urea denaturation was monitored by changes in CD ellipticity at 22 °C in buffer containing 30 mM Tris·HCl (pH 7.5), 0.1 M KCl, 10 mM $MgCl_2$, and 1.5 mM $CaCl_2$. For these assays, stocks of protein (at concentrations of either 4 or 12 μM) in 0 and 9 M urea were mixed to achieve the proper urea concentration, and samples were equilibrated until the CD signal stabilized. This occurred in less than 30 s for the N_{1-51} fragment but took 5−60 min for Mnt and the C-terminal fragments depending on the urea concentration. Thermal denaturations of proteins at concentrations from 5 to 40 μM in phosphate buffer were also monitored by changes in CD ellipticity. Thermal melts for the C-terminal fragments were reversible, but those for intact Mnt and the N_{1-51} fragment were not. Stability data were fit to different equilibrium models using nonlinear least-squares fitting using either a MacIntosh or Unix version of the program NONLIN (Johnson & Frasier, 1985; Brenstein, 1989). The equations used to fit denaturation data to a dimer−unfolded monomer equilibrium can be found in Milla *et al.* (1993). For equilibria involving tetramer−unfolded monomer or tetramer−dimer−unfolded monomer models, the concentrations of all species at a specified total protein concentration were solved by numerical approximation.

Analysis of Oligomeric Structure. Sedimentation equilibrium centrifugation experiments were performed at 22 °C using a Beckman XL-A analytical ultracentrifuge at rotor speeds of 15 000, 20 000, or 30 000 rpm. For these experiments, either SB buffer or SB buffer containing urea was used except for the N_{1-51} fragment for which PB buffer was used. Weight-average molecular weight values (M_a) were calculated by nonlinear least-squares fitting of the data, using NONLIN, to the function

$$\mathrm{Abs}_{(x)} = \mathrm{ABS}_{(x_f)} \exp[M_a(\omega^2/2RT)(1 - \nu\rho)(x^2 - x_f^2)]$$

where $\mathrm{Abs}_{(x)}$ and $\mathrm{Abs}_{(x_f)}$ are absorbances at radius x and at reference radius x_f, respectively, ω is the angular velocity, R is the gas constant, T is the temperature, ν is the partial specific volume calculated from the amino acid sequence, and ρ is the density of the solution (Laue *et al.*, 1992).

For cross-linking experiments, a stock solution of the bifunctional reagent dithiobis(succinimidyl propionate) (DSP) was prepared by dissolving 5 mg of DSP in 1 mL of dimethyl sulfoxide. Mnt (25 μM), N_{1-51} (25 μM), or C_{47-82} (200 μM) were incubated with a 10-fold molar excess of DSP in PB for 15 min at 22 °C. The cross-linking reactions were quenched by adding 3 mM lysine plus 25 mM Tris·HCl (pH 8.0) and were analyzed by SDS gel electrophoresis.

Operator Fragments and DNA Binding. DNA fragments for gel mobility shift assays and DNase I footprinting were generated by the polymerase chain reaction (PCR) using kinased primers and plasmid templates. Only one primer was end-labeled with ^{32}P, resulting in labeling of either the top or bottom strand. pMS200 (Youderian *et al.*, 1982) was used as the template for a 200-bp fragment containing the whole *mnt* operator. A derivative of pBluescript SK+ (Stratagene), with the sequence 5′-ATAGGTCCACGC-3′ cloned between *Eco*RI and *Bam*HI sites in the polylinker region, was used as the template for a 178-bp fragment containing the left *mnt* half-operator site.

Gel mobility shift experiments using a DNA concentration of ≈10 pM were performed largely as described (Knight & Sauer, 1988; Brown *et al.*, 1990) with two exceptions. First, reactions were incubated in a binding buffer containing Tris/potassium glutamate and 10% polyacrylamide gels were used for separation of bound and unbound DNA fragments. Second, Mnt was diluted from a 4.5 M urea buffer, in which it is an unfolded monomer, to allow full equilibration between the different oligomeric forms of Mnt. Binding reactions were incubated for at least 2 h at 22 °C. DNase I footprinting experiments were performed as described (Smith & Sauer, 1995). Protein was preincubated with end-labeled DNA (≈200 and ≈450 pM for whole- and half-operator fragments, respectively) for 2 h at 22 °C in footprinting buffer. DNase I was added to a final concentration of 125 ng/mL and after 1 min at 22 °C the reaction was quenched by the addition of 2.5 M ammonium acetate, 20 mM EDTA, and 10 μg/mL salmon sperm DNA. Under these conditions, the majority of end-labeled DNA remained uncleaved, indicating that the cleavage kinetics are single hit. Reactions were extracted with phenol/chloroform, ethanol precipitated, washed with 75% ethanol, dried, and resuspended in loading buffer. The radioactivity was quantified by Cherenkov counting, and equal numbers of counts of each sample were loaded onto 6% polyacrylamide/8.3 M urea denaturing gels. The intensities of bands in the operator region were quantified by phosphorimaging; to calculate fractional protection factors, operator intensities were normalized by dividing by the intensities of non-operator bands.

DNA-binding data were fit to different equilibrium models and values of K_{app} using NONLIN. For the N domain, concentrations of monomer ($[U] = (-K_u + \sqrt{K_u^2 + 8P_tK_u})/4$) and dimer ($[N_2] = (P_t - [U])/2$) were calculated from the total protein concentration (P_t) and the equilibrium constant for dimer dissociation (K_u). The fractional occupancy of the half-operator was calculated as $[N_2]/(K_{app} + [N_2])$. The fractional occupancy of the whole-operator was calculated as $[N_2]^2/(K_{app} + [N_2]^2)$. The latter equation ignores the concentration of dimer-bound operator, but this value is very small because of dimer−dimer cooperativity.

RESULTS

As part of this work, a variant of Mnt (Mnt-st6) with six additional C-terminal histidine residues was constructed. Synthetic or proteolytic fragments discussed here are named by their position in the Mnt-st6 sequence. Thus, N_{1-51} is an N-terminal fragment consisting of residues 1−51, while C_{52-88} is a C-terminal fragment consisting of residues 52−88. The positions of the different fragments studied here in relation to the Mnt-st6 sequence are diagrammed in Figure 1.

Domain Structure. To test for the presence of independent structural domains, Mnt and the Mnt-st6 variant were subjected to limited proteolysis with chymotrypsin. In both cases, cleavage produced two major fragments as assayed by SDS gel electrophoresis (see Figure 2 for the Mnt-st6 cleavage pattern). The larger cleavage fragment of Mnt had the same gel mobility as that of Mnt-st6; the smaller fragment from Mnt migrated at a faster rate than that of Mnt-st6 (data not shown). Since the two proteins differ only at their C termini, these results suggest that the smaller chymotryptic fragment is a C-terminal fragment. The chymotryptic fragments of Mnt-st6 were purified and subjected to amino

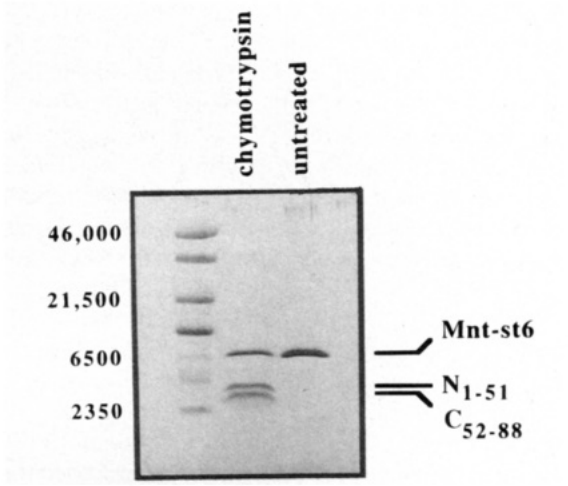

FIGURE 2: SDS gel electrophoretic analysis of Mnt-st6, Mnt-st6 cleaved with chymotrypsin, and molecular weight standards.

acid analysis and to N-terminal sequencing by the Edman degradation. The larger fragment (N_{1-51}) contained 51 residues and had the same N-terminal sequence as intact Mnt, NH_2-Ala-Arg-Asp-Asp-Pro-His-Phe-Asn-Phe-Arg-Met-Pro; the smaller fragment (C_{52-88}) contained 37 residues and had the N-terminal sequence NH_2-Arg-Asn-Asp-Ala-Glu-Arg-Leu-Ala-Asp-Glu-Gln. These results indicate that the two fragments arise from a single chymotryptic cleavage between Tyr^{51} and Arg^{52} (see Figure 1).

Prior to the analysis of the proteolytic experiments described above, a peptide corresponding to residues 47–82 of Mnt was synthesized (C_{47-82}). Compared to the C_{52-88} fragment, the synthetic peptide lacks the His6 tag at the C terminus and contains five additional amino acids at the N terminus (see Figure 1). The former residues are not present in wild-type Mnt, and the latter residues, which seem to be part of an intradomain linker in the intact protein, are unstructured in Mnt_{1-76} (Burgering *et al.*, 1994). Because the synthetic C_{47-82} peptide was available in larger quantities than the C_{52-88} fragment, it was used for many of the subsequent experiments. As discussed below, the C_{47-82} peptide also has a more stable oligomeric structure and a higher α-helical content than the C_{52-88} fragment.

Oligomeric Structure. The oligomerics of Mnt and the proteolytic or synthetic fragments were assayed by equilibrium sedimentation centrifugation and by cross-linking experiments. As expected from previous studies (Vershon *et al.*, 1985), intact Mnt appears to be largely tetrameric on the basis of its sedimentation properties at concentrations from 2.5 to 25 μM (Table 1) and also cross-links to give dimers, trimers, and tetramers (lane F, Figure 3). N_{1-51} has an apparent molecular weight closest to that expected for a dimer in sedimentation experiments (Table 1) and cross-links to a dimer but not to higher species (lane D, Figure 3). The C_{47-82} fragment sediments with an average molecular weight that increases from one expected for dimer at 10 μM to one approaching tetramer at 200 μM (Table 1). Cross-linking of the C_{47-82} fragment yields species corresponding to dimers, trimers, and tetramers, but not higher species (lane B, Figure 3). Hence, the C_{47-82} fragment appears to form tetramers which are in equilibrium with dimers (and possibly monomers as well) at concentrations from 10 to 200 μM. For both the C_{47-82} fragment and intact Mnt, the relative band intensities of the cross-linked species (tetramer > dimer > trimer, 4° > 2° > 3°) suggest that the tetramers have a dimer of dimers structure (see Discussion).

Table 1: Oligomeric State of Mnt and N- and C-Domain Fragments[a]

protein	concn	M_a[b]	M_a/M_r[c]	major cross-linked species
Mnt	2.5 μM	33 265 (±642)	3.48	
	10 μM	33 851 (±485)	3.54	
	25 μM	35 986 (±228)	3.76	2°, 3°, 4°
	25 μM, 3 M urea	26 001 (±484)	2.72	2°, 3°, 4°
N_{1-51}	4 μM	9 430 (±176)	1.60	
	10 μM	9 240 (±177)	1.57	
	20 μM	8 959 (±70)	1.52	2°
C_{47-82}	10 μM	8 100 (±185)	1.96	
	50 μM	13 200 (±120)	3.13	
	200 μM	14 380 (±55)	3.42	2°, 3°, 4°
C_{52-88}	10 μM	6 717 (±139)	1.48	
	50 μM	10 965 (±146)	2.43	2°, 3°, 4°

[a] Sedimentation and cross-linking experiments were performed at 22 °C, pH 7.5 in PB or SB buffer. [b] Average molecular weight (±sd) calculated from equilibrium sedimentation centrifugation using a single species function (see Materials and Methods). [c] M_a divided by M_r, the monomer molecular weight calculated from amino acid sequence. M_r values: Mnt (9548), N_{1-51} (5879), C_{47-82} (4204), C_{52-88} (4510).

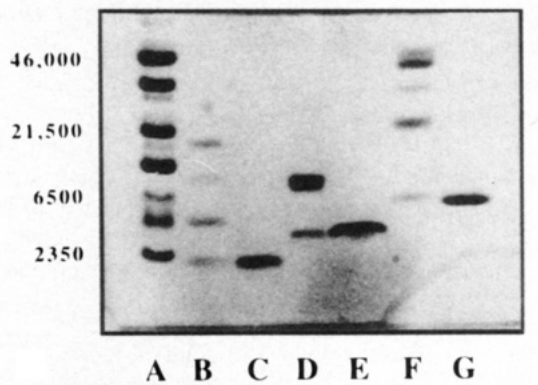

FIGURE 3: SDS gel electrophoretic analysis of proteins before and after cross-linking with dithiobis(succinimidyl propionate). Lanes: A, molecular weight standards; B, peptide C_{47-82} following cross-linking; C, untreated C_{47-82}; D, fragment N_{1-51} following cross-linking; E, untreated N_{1-51}; F, Mnt following cross-linking; G, untreated Mnt. The apparent anomalies in the electrophoretic mobilities of some low molecular weight standards and cross-linked species probably result from sequence specific variations in the amount of bound SDS and/or in the shape of the SDS–peptide complex. In the cross-linking reactions shown in lanes B, D, and F, the observation of monomers, dimers, and trimers for Mnt and C_{47-82} and of monomers for N_{1-51} probably results from incomplete reactions caused by hydrolysis of one of the functional groups on the bifunctional cross-linking reagent and should not be taken as evidence that such species are significantly populated in solution.

Secondary Structure and Stability. Mnt, N_{1-51}, and C_{47-82} are all predominantly α-helical as shown by their circular dichroism (CD) spectra which have peaks of negative ellipticity near 222 and 208 nm (Figure 4a). Moreover, addition of the CD spectra of the N_{1-51} and C_{47-82} fragments gives a spectrum-similar to that of intact Mnt (Figure 4a), suggesting that the α-helical structures of the isolated domains are representative of these domains in the intact protein. The CD spectrum of C_{52-88} showed less than one-half of the α-helical content of C_{47-82} (data not shown). This difference may arise because the C_{52-88} peptide is less tetrameric than the C_{47-82} peptide at similar concentrations

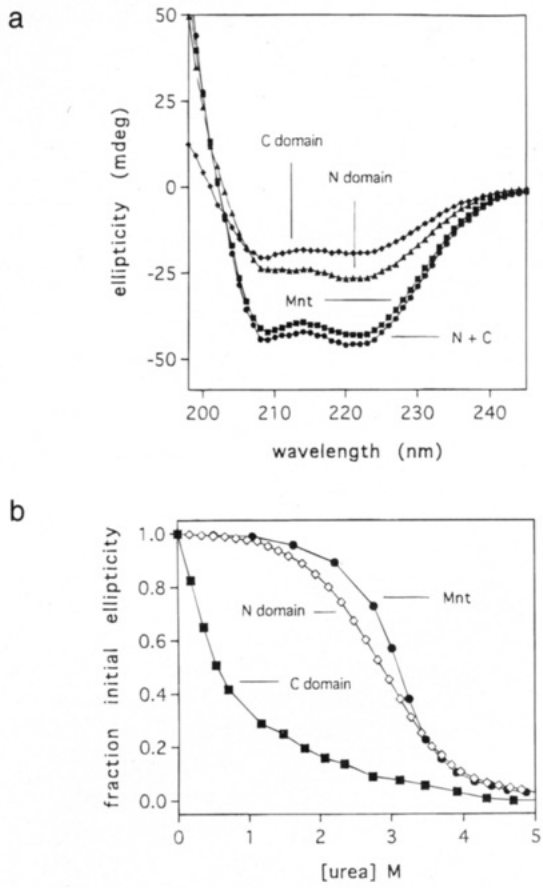

FIGURE 4: (a) Circular dichroism spectra of the C domain (peptide C_{47-82}), the N domain (fragment N_{1-51}), and intact Mnt. All spectra were taken at 25 °C in PB buffer, using a 0.1 cm cuvette, at protein or peptide concentrations of 38.6 μM. Addition of the C- and N-domain spectra (labeled N + C) gives a spectrum similar to that of Mnt. (b) Urea denaturation of the C domain (peptide C_{47-82}), the N domain (fragment N_{1-51}), and intact Mnt. Experiments were performed using 12 μM protein or peptide, at 22 °C in buffer containing 30 mM Tris·HCl (pH 7.5), 0.1 M KCl, 10 mM $MgCl_2$, and 1.5 mM $CaCl_2$.

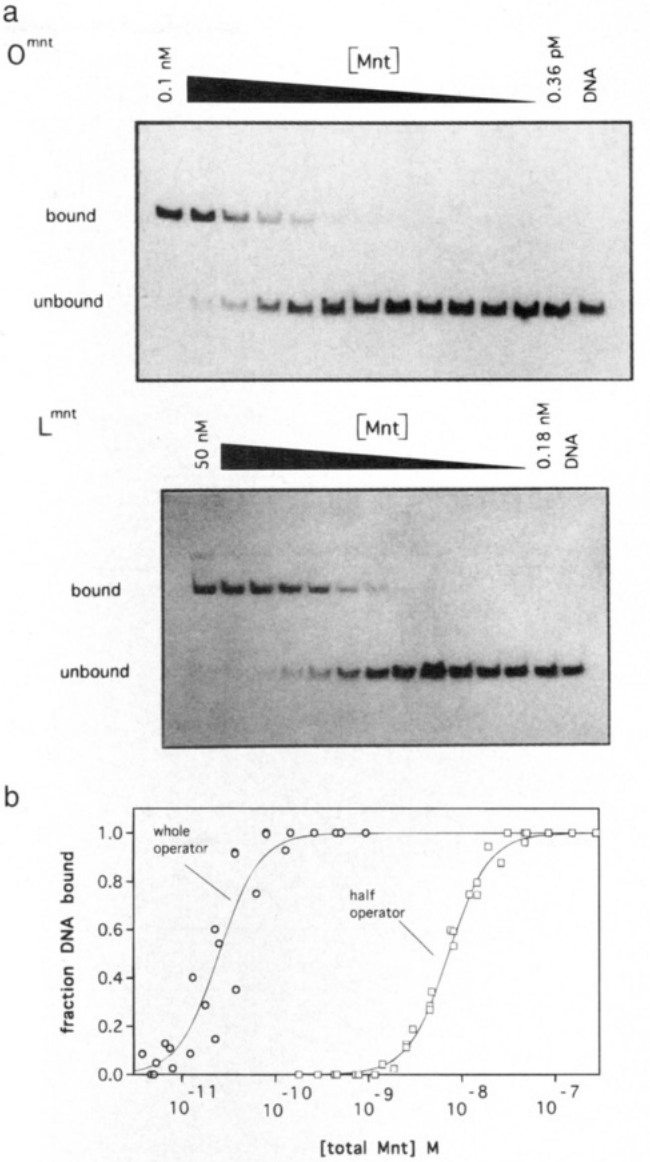

FIGURE 5: (a) Gel mobility shift assays of the binding of Mnt to DNA fragments containing the whole 21-base-pair *mnt* operator (top) or an 11-base-pair *mnt* operator half-site (bottom). In both gels, the rightmost lane contains DNA without added protein and the concentration of Mnt increases from right to left in equal increments. Incubations were performed at 22 °C in a buffer containing 30 mM Tris·HCl (pH 7.5), 0.1 M potassium glutamate, 10 mM $MgCl_2$, 1.5 mM $CaCl_2$, 0.1 mM EDTA, 100 μg/mL bovine serum albumin, and 0.02% Nonidet P-40. (b) Binding curves. Data points are from three independent experiments for both the whole- and half-operator experiments. The Mnt concentration is the free protein concentration in total monomer equivalents. The solid lines are theoretical curves for the dissociation of a tetrameric protein–DNA complex to two free dimers and free DNA with equilibrium constants of 2.3×10^{-22} M^2 (whole-operator) and 1.3×10^{-17} M^2 (half-operator).

(see Table 1), and/or may indicate that the C_{52-88} tetramer has less α-helix than the C_{47-82} tetramer.

In urea denaturation studies, Mnt and fragments N_{1-51} and C_{47-82} showed melts indicative of cooperatively folded, three-dimensional structures (Figure 4b). The α-helical structure of the C_{47-82} fragment is the least stable to denaturation, while that of the N_{1-51} fragment is only slightly less stable than intact Mnt. Because Mnt is more stable than either fragment alone and denatures in a monophasic fashion, it appears that the N and C domains help to stabilize each other and unfold coincidently in the intact protein.

The urea denaturation experiments shown in Figure 4b were performed at protein concentrations of 12 μM. For Mnt and the N_{1-51} fragment, denaturation experiments were also performed at 4 μM. In both cases, the proteins were less stable to denaturation at the lower concentration (data not shown), indicating that oligomer dissociation is coupled to protein unfolding. Simultaneous nonlinear least-squares fitting of the 4 and 12 μM data for the N_{1-51} fragment gave an excellent fit to a model in which a folded dimer is in equilibrium with two unfolded monomers ($K_u(H_2O) = 1.01 \times 10^{-8}$ M; $\Delta G_u(H_2O) = 10.75$ (±0.13) kcal/mol; $m = 1.54$ (±0.05) kcal/mol·M). The 4 and 12 μM data for denaturation of intact Mnt could be fit to within experimental error by a variety of equilibrium models (dimer–unfolded monomer; tetramer–unfolded monomer; tetramer–dimer–unfolded monomer). It is unlikely that the dimer–monomer model is correct because cross-linking experiments indicate that Mnt tetramers persist at urea concentrations within the denaturation transition zone (Table 1). We favor a tetramer–dimer–unfolded monomer dissociation model, in part because Mnt_{1-76} is known to be dimeric (Knight & Sauer, 1988; Burgering *et al.*, 1994). The available data do not, however, permit derivation of unambiguous equilibrium constants for either elementary reaction (i.e., tetramer dissociation to two

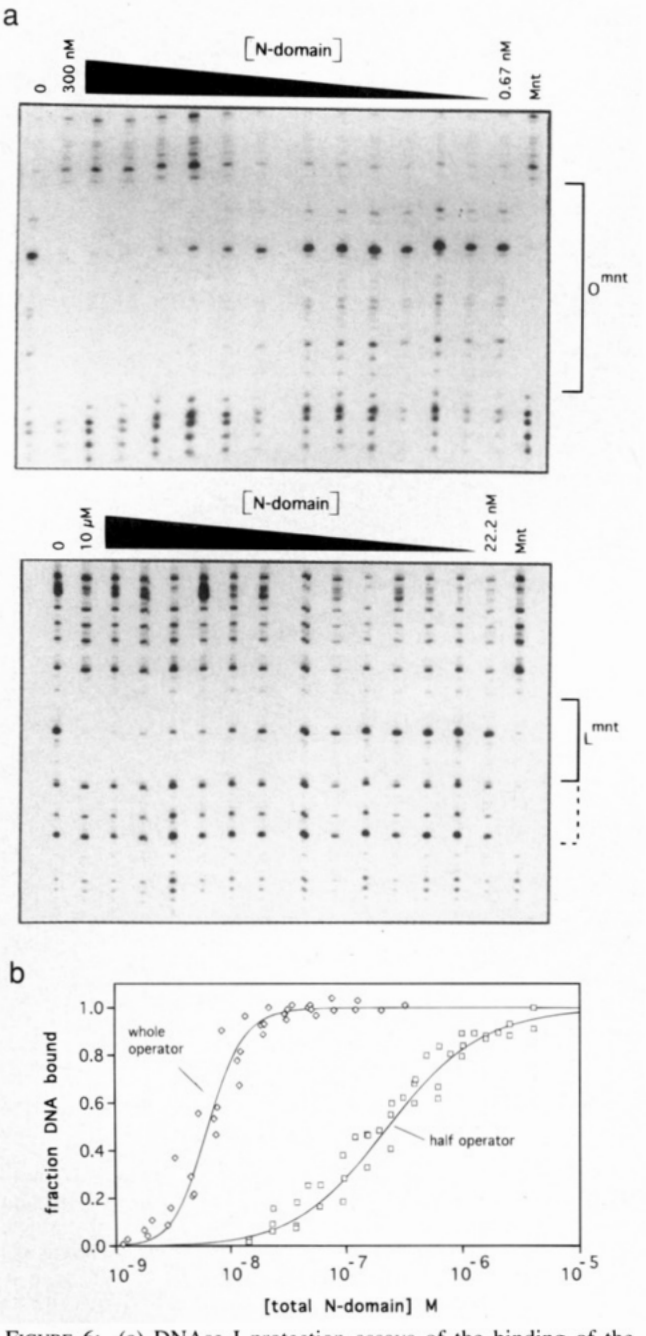

FIGURE 6: (a) DNAse I protection assays of the binding of the N_{1-51} fragment to operator DNA (O^{mnt}; top gel) and half-operator DNA (L^{mnt}; bottom gel). In both gels, the rightmost lane shows the protection pattern obtained with 25 nM Mnt and the concentration of N domain increases from right to left in equal increments. (b) Binding curves. Data points are from 3 to 4 independent DNase I protection experiments. The N-domain concentration is in total monomer equivalents. The solid line for whole-operator binding is a theoretical curve calculated for dissociation of a tetrameric protein−DNA complex to two free dimers and free DNA ($K_{app} = 1.8 \times 10^{-18}$ M^2) with subsequent dissociation of dimers to unfolded monomers ($K_u = 1.0 \times 10^{-8}$ M). The solid line for half-operator binding is a theoretical curve calculated for dissociation of a dimeric protein−DNA complex to free dimer and free DNA ($K_{app} = 9.9 \times 10^{-8}$ M) with subsequent dissociation of the dimer to unfolded monomers ($K_u = 1.0 \times 10^{-8}$ M).

dimers or dimer dissociation to two unfolded monomers) in this model.

Operator DNA Binding. In gel mobility shift experiments, half-maximal binding of intact Mnt to the *mnt* operator to form the tetrameric protein−DNA complex occurs at a protein concentration of approximately 20 pM (Figure 5). Although there is reasonable scatter, these binding data show an approximate second-order dependence on protein concentration (Hill constant = 2.02 ± 0.32; $r = 0.84$). First- and fourth-order reactions, respectively, would be expected if Mnt were fully tetrameric or monomeric at these low DNA-binding concentrations. The observed second-order dependence indicates the existence of a significant population of free dimers but does not rule out that these species are also in equilibrium with smaller quantities of monomer and/or tetramer.[1]

We were unable to detect operator binding of the N_{1-51} fragment in DNA mobility shift experiments, possibly because the complex dissociates too rapidly to allow separation of bound complexes and free DNA. In DNase I footprinting assays (Figure 6a, top panel), however, the N_{1-51} fragment shows the same protection pattern as intact Mnt and gives half-maximal protection of the *mnt* operator at a protein concentration of roughly 6 nM. Thus, binding of the N-terminal domain dimer to the *mnt* operator appears to be 3−4 orders of magnitude weaker than binding of the Mnt dimer to this operator. As shown in Figure 6b, the N_{1-51}−operator-binding curve is fit well by a model in which the apparent equilibrium constant for dissociation of the tetrameric operator complex to give free operator and two N_{1-51} dimers is 1.8×10^{-18} M^2.

The DNA-binding experiments described above were performed using the 21-base-pair *mnt* operator, which is composed of nearly identical half-sites (Vershon *et al.*, 1987a). DNA mobility shift (Mnt; Figure 5a, bottom panel) and footprinting experiments (N_{1-51}; Figure 6a, bottom panel) were also performed using a DNA fragment containing just a single half-site of the *mnt* operator, since comparison of whole and half-operator binding allows analysis of potential cooperative interactions between DNA-bound dimers. Compared with binding of each protein to the intact operator, roughly 250-fold higher concentrations of Mnt and 30-fold higher concentrations of the N_{1-51} fragment were required to achieve comparable levels of binding to the half-site (Table 2; Figures 5b and 6b). This indicates that binding of either Mnt dimers or N_{1-51} dimers to each half-site in the intact *mnt* operator is cooperative. In the case of Mnt, cooperativity is also indicated by the absence of dimer−operator intermediates in the DNA mobility shift experiments (Figure 5a).

Mnt binds to the half-site DNA at lower concentrations than the N_{1-51} fragment (compare Figures 5b and 6b). The Mnt dimer might make more DNA contacts than the N_{1-51} dimer, for example if the C domain contacted operator DNA directly. This interpretation, however, seems inconsistent with the observation that footprints of Mnt and N_{1-51} on the intact operator are identical. It is also possible that the Mnt species bound to half-site DNA is a tetramer, with one dimer binding to the operator half-site and the other interacting with adjacent DNA nonspecifically. We favor this second interpretation for two reasons. First, as shown in the leftmost lane of the bottom panel of Figure 6a, there is some protection of the DNA next to the L1 half-site in the DNase I footprint produced by Mnt, consistent with nonspecific

[1] Studies performed by Vershon *et al.* (1987a) suggested that Mnt was tetrameric at DNA-binding concentrations. Here, we find that Mnt is largely dimeric at DNA-binding concentrations. This difference may result from the use of different binding buffers or procedures for adding Mnt to DNA in the two studies.

Table 2: Binding of N_{1-51} and Mnt to Operator and Half-Operator DNA

protein−DNA complex	[protein] at half-maximal binding[a] (M)	equilibrium model[b]	equilibrium constant[c]
N_{1-51}−operator	6.4×10^{-9}	$N_4O \rightleftarrows 2N_2 + O$	$1.8 (\pm 0.8) \times 10^{-18}$ M^2
N_{1-51}−half-site	2.1×10^{-7}	$N_2H \rightleftarrows N_2 + H$	$9.9 (\pm 2.6) \times 10^{-8}$ M
Mnt−operator	2.3×10^{-11}		
Mnt−half-site	7.3×10^{-9}		

[a] Free protein concentration in monomer equivalents required for half-maximal binding of the 200-bp whole-operator fragment (O1) or the 178-bp half-operator fragment (L1) determined by DNA mobility shift experiments for Mnt and by DNase I footprinting experiments for the N_{1-51} fragment (see Figures 5 and 6). Assays were performed at pH 7.5, 22 °C, in 30 mM Tris or 30 mM HEPES buffer containing 0.1 M potassium glutamate, 10 mM $MgCl_2$, 1.5 mM $CaCl_2$, 0.1 mM EDTA, 100 μg/mL bovine serum albumin, and 0.02% Nonidet P-40. [b] Equilibrium models used to fit binding data. For the N_{1-51} fragment, dimer concentrations were calculated using a dimer dissociation/unfolding constant of 1.0×10^{-8} M, the value determined from urea denaturation experiments. [c] Equilibrium constants for the model shown were determined by nonlinear least-squares fitting of the binding data shown in Figure 6b. Equilibrium constants were not calculated for the Mnt-binding reactions because the relevant equilibrium constants for oligomerization are not known.

protection by a second Mnt dimer. Second, as shown in Figure 5b, the Mnt binding curves for the half- and whole-operator DNA fragments are offset but roughly parallel, as would be expected if the reactions were second order and the bound species were tetrameric in both cases. By contrast, the curve for N_{1-51} binding to whole-operator DNA is steeper than the curve for half-operator DNA (Figure 6b), as expected if tetramers are the species bound to the whole operator and dimers are the species bound to the half-operator.

DISCUSSION

The experiments presented here show that Mnt contains two functional domains. The N domain forms dimers that bind operator DNA weakly, but specifically and cooperatively. The C domain forms tetramers and, in the context of the intact protein, enhances the DNA binding of the N domains significantly (Table 2). Thus, like many DNA-binding proteins, Mnt has a modular design. An N-terminal, dimeric domain is responsible for site-specific DNA recognition, and a second, C-terminal tetramerization domain is necessary for strong DNA binding.

The properties of the N domain (residues 1−51) of Mnt are very similar to those of the homologous Arc repressor of phage P22. Both are folded as dimers with each monomer consisting of a β-ribbon−helix−helix fold. Each binds to a 21-base pair operator as a tetramer, with dimers binding to individual half-sites. The N_{1-51} dimer binds to an operator half-site with a half-maximal concentration of roughly 200 nM. If the adjacent half-site is occupied by another N_{1-51} dimer, however, then the protein concentration required for half-maximal binding decreases to 6 nM. This indicates that adjacently bound N-domain dimers interact cooperatively. This type and magnitude of dimer−dimer cooperativity is also seen in the binding of Arc to operator DNA (Brown & Sauer, 1993). In the Arc−operator complex, dimer−dimer cooperativity is largely mediated by a set of cross-dimer hydrogen bonds between Arg^{31} and the polypeptide main chain of the adjacent dimer (Raumann *et al.*, 1994; Waldburger *et al.*, 1995). In the Mnt−operator complex, Arg^{29} (the homolog of Arg^{31} in Arc; Figure 1) could mediate similar interactions between adjacently bound Mnt dimers. Intact Mnt, however, binds operator DNA significantly more strongly than the N_{1-51} fragment (Table 2). Because there is no evidence that the C domain makes direct DNA contacts, this suggests that linking two N-domain dimers via interactions mediated by the C domain provides an additional level of cooperativity that stabilizes the Mnt−operator complex.

Several observations indicate that the C-terminal 30−35 residues of Mnt comprise an independent tetramerization domain. First, peptide C_{47-82} is α-helical and has a CD spectrum extremely close to that expected for residues 52−82 in intact Mnt. Second, this peptide shows cooperative denaturation, as expected for a domain with a defined tertiary structure. Third, C_{47-82} forms tetramers in cross-linking experiments and at concentrations from 10 to 200 μM appears to be an equilibrium mixture of tetramers and dimers. Intact Mnt is tetrameric, but deletion of the C domain, as shown here, or even the last 6−7 residues of this domain (Knight & Sauer, 1988) results in dimeric variants. Hence, the ability of the protein to form tetramers appears to reside exclusively in the C-terminal domain. The N and C domains of Mnt do, however, influence each other. Thus, tetramers of Mnt are more stable than tetramers of the C domain by itself, and both the N and C domains are more resistant to denaturation in the intact protein than as isolated fragments. One simple explanation for these observations is that dimerization of the N domain helps stabilize C-terminal tetramerization by increasing the effective concentration of C-terminal regions and *vice versa*. Alternatively, there may be contacts between the N domain and C domain that contribute directly to the mutual stabilization. Similar mechanisms presumably account for the ability of the C domain to enhance operator binding. The C domain could help orient both N-terminal dimers for operator binding or increase the effective concentration of the N-domain dimers so that binding of one dimer to a half-site makes binding of the second dimer entropically more favorable.

At present, almost nothing is known about the structural organization of the C domain in the intact Mnt tetramer. NMR studies of the dimeric Mnt_{1-76} variant show the presence of α-helices from residues 54−66 and 54′−66′ followed by a disordered region extending to the C terminus (Burgering *et al.*, 1994). Somewhat surprisingly, however, these C-terminal helices pack back against the N domain in the 1−76 structure and do not interact significantly with each other. This could mean that the C terminal helices only interact in the Mnt tetramer or that the positions of these helices in the mutant dimer are an artifact of the deletion of key residues important for helix−helix interactions. The CD spectra of the C_{47-82} peptide indicates roughly 40% helix, and the tetrameric nature of this fragment makes some type of four-helix bundle a possibility. p53, the human tumor-suppressor DNA-binding protein, also contains a small, C-terminal, tetramerization domain (Pavletich *et al.*, 1993), which forms an antiparallel four-helical bundle (Sakamoto *et al.*, 1994; Jeffrey *et al.*, 1995).

There are only two ways to form a symmetric tetrameric protein that will not participate in further oligomerization. One is a dimer or dimers arrangement with three, mutually perpendicular 2-fold axes (D_2 or 222 symmetry). The other is by having each subunit occupy an equivalent position related to the next by a 90° rotation about a single 4-fold

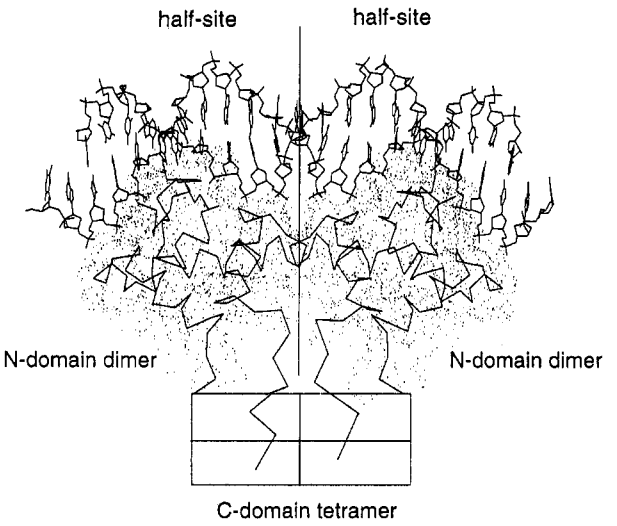

FIGURE 7: Model for the Mnt–operator complex. The interactions of the two N-domain dimers with operator DNA half-sites and with each other are modeled from the cocrystal structure of the Arc–operator complex (Raumann *et al.*, 1994). The C-domain tetramer and links to the N domains are shown schematically. The dotted surface represents the solvent accessible surface of the N domain, calculated for residues 1–51 of Mnt_{1-76} (Burgering *et al.*, 1994).

symmetry axis (C_4 symmetry). In cross-linking studies, a C_4 tetramer would be expected to display a 4° > 3° > 2° or a 4° < 3° < 2° order of band intensities depending upon the inherent efficiency of the cross-linking reaction. The cross-linking results for both Mnt and the C_{47-82} fragment, however, show a 4° > 2° > 3° order of band intensities (lanes B and F, Figure 3) and are thus more consistent with a dimer of dimers symmetry arrangement. The same conclusion has been reached based on preliminary NMR studies of intact Mnt (Burgering *et al.*, 1994). This, however, raises an interesting problem because the Mnt tetramer–operator complex can not have D_2 symmetry (or C_4 symmetry for that matter). When bound to the operator, the 2-fold axes of each N-domain dimer need to be roughly parallel to each other to make the proper DNA contacts. This could be accomplished if the N-domain dimers were connected to a D_2 symmetric C-domain tetramer via flexible linker regions (Figure 7), giving rise to a system with mixed symmetry. Another striking example of a protein–DNA interaction in which the symmetry of an oligomerization domain is fundamentally mismatched to the symmetry of binding site occurs in the yeast heat shock transcription factor, where the protein is a trimer (Sorger & Nelson, 1989). This symmetry mismatch is also overcome by using flexible linker regions to connect the oligomerization domain to the DNA-binding domains (Flick *et al.*, 1994).

Why does Mnt have a structurally distinct tetramerization domain? Tetramer formation in solution is not required for DNA binding *per se* as both the dimeric N domain of Mnt and the dimeric Arc repressor bind DNA specifically and yet only form tetramers when bound to DNA. Mnt and Arc are responsible for repression of the *antirepressor* operon during lysogenic and lytic growth, respectively (Susskind & Youderian, 1983). Mnt must efficiently shut off expression of Antirepressor protein which would otherwise inactive the *c*2 repressor, resulting in induction of the resident prophage. Conversely, Arc need only dampen transcription during lytic growth to prevent the overaccumulation of Antirepressor protein which would otherwise inhibit phage growth (Susskind & Botstein, 1980). Because stable repression is more important for Mnt than for Arc, Mnt probably needs to bind to its operator DNA significantly more strongly than does Arc. Indeed, under comparable conditions, Mnt binds to its operator about 10-fold more avidly than Arc (Brown *et al.*, 1990). Mnt seems to have achieved stronger operator binding than Arc by employing a separate tetramerization domain to link the binding energies of its Arc-like, dimeric DNA-binding domains.

ACKNOWLEDGMENT

We thank Tracy Smith, Brigitte Raumann, Bronwen Brown, Joel Schildbach, and Tania Baker for materials, advice, and help.

REFERENCES

Amman, E., Brosius, J., & Ptashne, M. (1983) *Gene 25*, 167–178.
Bonvin, A. M. J. J., Vis, H., Breg, J. N., Burgering, M. J. M., Boelens, R., & Kaptein, R. (1994) *J. Mol. Biol. 236*, 328–341.
Breg, J. N., van Opheusden, J. H. J., Burgering, M. J. M., Boelens, R., & Kaptein, R. (1990) *Nature 346*, 586–589.
Brenstein, R. J. (1989) *Robelko Software, version 0.9 8b5*, Carbondale, IL.
Brown, B. M., & Sauer, R. T. (1993) *Biochemistry 32*, 1354–1363.
Brown, B. M., Bowie, J. U., & Sauer, R. T. (1990) *Biochemistry 29*, 11189–11195.
Burgering, M. J. M., Boelens, R., Gilbert, D. E., Breg, J. N., Knight, K. L., Sauer R. T., & Kaptein, R. (1994) *Biochemistry 33*, 15036–15045.
Chen, Y.-H., Yang, J. T., & Martinez, H. M. (1972) *Biochemistry 11*, 4120–4131.
Fasman, G. D. (1975) *Handbook of Biochemistry and Molecular Biology, Vol. 1, Proteins*, CRC Press, Cleveland, OH.
Flick, K. E., Gonzalez, L., Jr., Harrison, C. J., & Nelson, H. C. M. (1994) *J. Biol. Chem. 269*, 12475–12481.
Knight, K. L., & Sauer, R. T. (1988) *Biochemistry 27*, 2088–2094.
Knight, K. L., & Sauer, R. T. (1989) *Proc. Natl. Acad. Sci U.S.A. 86*, 797–801.
Laue, T. M., Shah, B. D., Ridgeway, T. M., & Pelletier, S. L. (1992) in *Analytical Ultracentrifugation in Biochemistry and Polymer Science* (Harding, S., Rowe, A., & Horton, J., Eds.) pp 90–125, Royal Society of Chemistry, Cambridge, U.K.
Johnson, M., & Frasier, S. (1985) *Methods Enzymol. 117*, 301–342.
Milla, M. E., Brown, B. M., & Sauer, R. T. (1993) *Protein Sci. 2*, 2198–2205.
Pavletich, N. P., Chambers, K. A., & Pabo, C. O. (1993) *Genes Dev. 7*, 2556–2564.
Raumann, B. E., Rould, M. A., Pabo, C. O., & Sauer, R. T. (1994) *Nature 367*, 754–757.
Sakamoto, H., Lewis, M. S., Hiroaki, K., Appella, E., & Sakaguchi, K. (1994) *Proc. Natl. Acad. Sci. U.S.A. 91*, 8974–8978.
Sauer, R. T., Krovatin, W., DeAnda, J., Youderian, P., & Susskind, M. M. (1983) *J. Mol. Biol. 168*, 699–713.
Schagger, H., & von Jagow, G. (1987) *Anal. Biochem. 166*, 368–379.
Smith, T. L., & Sauer, R. T. (1995) *J. Mol. Biol.* (in press).
Sorger, P. K., & Nelson, H. C. M. (1989) *Cell 59*, 807–813.
Susskind, M. M., & Botstein, D. (1980) *Virology 100*, 685–713.
Susskind, M. M., & Youderian, P. (1983) in *Lambda II* (Hendrix, R. W., Roberts, J. W., Stahl, F. W., & Weisberg, R., Eds.) pp 347–366, Cold Spring Harbor Press, Cold Spring Harbor, NY.
Vershon, A. K., Youderian, P., Susskind, M. M., & Sauer, R. T. (1985) *J. Biol. Chem. 260*, 12124–12129.
Vershon, A. K., Liao, S.-M., McClure, W. R., & Sauer, R. T. (1987a) *J. Mol. Biol. 195*, 311–322.
Vershon, A. K., Liao, S.-M., McClure, W. R., & Sauer, R. T. (1987b) *J. Mol. Biol. 195*, 323–331.
Waldburger, C. D., Schildbach, J. F., & Sauer, R. T. (1995) *Nature Struct. Biol. 2*, 122–128.
Youderian, P., Bouvier, S., & Susskind, M. M. (1982) *Cell 30*, 843–853.

BI9507387